

Modification of physical and structural properties of $\text{Bi}_{1.8}\text{Pb}_{0.4}\text{Sr}_2\text{Ca}_{2.2}\text{Cu}_3\text{O}_y$ ceramics induced by annealing

Berdan Özkurt^{a,*}, M. A. Madre^b, A. Sotelo^b, J. C. Diez^b

^a Department of Energy Systems Engineering, Faculty of Tarsus Technology, University of Mersin, Mersin, Turkey

^b ICMA (CSIC-Universidad de Zaragoza), María de Luna, 3. 50018 Zaragoza, Spain

Abstract

The effect of annealing temperatures on the structural and superconducting properties of Bi-2223 ceramics prepared by solid state reaction method has been investigated. Annealing temperatures were varied from 730 to 830 °C while time was kept constant at 50 h. Electrical resistivity studies showed that samples annealed at 830 °C for 50 h have the lowest resistivity values at room temperature while critical transition temperature increases slightly. XRD data have shown that all samples contain Bi-2223 as the major one. The highest diamagnetism behaviour has been found in the sample treated at 830 °C. In addition, J_c values of the samples, calculated from the hysteresis loops using the Bean's model, decreased with increasing annealing temperatures until 780 °C and increase for the highest annealing temperature which is 830 °C for this work.

Keyword: Bi-2223; XRD; Electrical resistivity; hysteresis loops

* Corresponding author. Tel.: +90 324 627 4804; fax: +90 324 627 4805

E-mail address: berdanozkurt@mersin.edu.tr

1. Introduction

Since the discovery of Bi-based high-temperature superconductors [1], one of the most important aims has been to increase the current transport capacity of these materials. The first step has been centered in the preparation of homogeneous precursors to obtain nearly pure phase materials. These materials were mainly obtained via solution methods which avoid the inhomogeneities inherent to the classical solid state synthesis [2-5]. These bulk materials have shown that the homogeneity was not enough to produce materials with high electrical current transport capacity [6]. As a consequence, many works have been performed in order to obtain high electrical capacity materials. Most of them were based on the grain orientation with the transport direction and the improvement of the grain links. Many processes have shown to be useful to produce high electrical density (but usually low current intensity) carrying materials, such as thin films [7], cables or tapes [8]. On the other hand, other processes are useful to produce bulk materials with high electrical current transport properties, such as hot-forging [9], microwave texturing [10], laser floating zone (LFZ) [11], or the new electrically assisted laser floating zone (EALFZ) technique [12].

The main drawback of such materials was the important decrease on the current transport capacity when subjected to external applied fields or even at self-field due to the flux lines movement in the mixed state. Nowadays it is well known that pinning centres act as a barrier against magnetic flux lines movement and, as a consequence, higher critical current density values can be reached. These pinning centres are crystalline defects and impurities which usually are isolating phases with small sizes [13] which can be easily generated

by several processes as, for example, neutron irradiation [14] or doping. There have been many studies on BSCCO ceramic doping to improve their critical transition temperature, critical current density and magnetic field carrying capacity. These works showed there have been important improvements in the superconducting properties when doping with some elements such as Li, Nb, B, Cd, Sn, Ag, Pb [15-27]. Other possibility to produce these pinning centers is based on the self-production of isolating phases with the adequate size to act as pinning centers. It has been demonstrated that it is possible to produce this effect on Bi-2212 phase using the phase diagram equilibrium [13,28]. In the case of Bi-2223 superconductor, it is well known that this phase is stable in a range of compositions [29] and temperatures [30] and it can be seen as a good candidate to perform its controlled decomposition to produce pinning centers. In the present work, the effect of annealing temperatures on the Bi-2223 phase and, as a consequence, on the properties of Bi-2223 ceramics, has been investigated. The changes on structural and superconducting properties produced in the samples subjected 50 h to different temperatures will be evaluated using X-ray powder diffraction (XRD), scanning electron microscopy (SEM), dc electrical-resistivity (R-T), and magnetic characterization.

2. Experimental

With the data obtained from the quasi-quinary phase equilibrium diagram [31], samples with $\text{Bi}_{1.8}\text{Pb}_{0.4}\text{Sr}_2\text{Ca}_{2.2}\text{Cu}_3\text{O}_y$ nominal composition were prepared by a conventional solid state reaction method from high purity Bi_2O_3 (Aldrich, 99 %), PbO_2 (Aldrich, 99.9 %), SrCO_3 (Aldrich, 99.9 %), CaCO_3 (Aldrich, 99.9 %), and CuO (Aldrich, 99.99 %) powders. They were weighed in the appropriate

proportions and mechanically mixed using an agate mortar. After milling process, the mixture was calcined at 750 °C for 12 h and milled in a grinding machine for 2 hours to obtain better homogeneous mixture. Then the powder was calcined again at 820 °C for 12 h to decompose the alkaline earth carbonates and start the formation of the different intermediate phases. The calcinations at 820 °C for all samples and grinding procedures were repeated three times to produce the reaction between the intermediate phases to start producing the superconducting Bi-2223 phase. After calcination process, the resulting powder was pressed into pellets of 13 mm diameter with an applied pressure of 375 MPa.

Finally, these green ceramics were sintered at 860 °C for 172 h in air to produce the Bi-2223 phase as the major one. Then, annealing processes were performed, during 50 h at different temperatures, on some of the samples while other ones were kept as reference after sintering procedure. Reference samples and those thermally treated at 730, 780, and 830 °C for 50 h, will hereafter be named A1, A2, A3, and A4, respectively.

X-ray powder diffraction analyses were performed in a Rigaku Ultima IV X-Ray Diffractometer in the range $2\theta = 3-60^\circ$ to determine the phases present in the samples. The surface morphologies were performed on representative samples in a Zeiss/Supra 55 Scanning Electron Microscopy (SEM). Resistivity and magnetic measurements were carried out on a Cryogenic Limited PPMS (from 5 to 300 K) which can reach the cryogenic temperatures about to 2 K in a closed-loop He system.

3. Results and discussion

Fig. 1 shows the powder XRD patterns obtained for all samples. From these data it is obvious that Bi-2223 phase is the major one in all cases, as reflected by its diffraction peaks (indicated by * in Fig. 1A1). The reference sample, (the unannealed one) A1, shows only small peaks belonging to the Bi-2212 secondary phase. This is a very important result when taking into account that the production of samples consisting in nearly pure Bi-2223 phase is a very difficult task, as can be deduced from the phase equilibrium diagram [31]. It clearly indicates that the synthesis procedure has been adequately chosen to obtain the Bi-2223 phase as the major one. When these sintered samples are annealed, two different evolutions can be observed. For samples annealed at low temperatures (A2 and A3), an increase on the Bi-2212 phase is produced, clearly indicated by the two new peaks appearing in the A2 and A3 diffraction patterns shown in Fig. 1. This effect is produced by a thermal treatment performed in conditions far from the Bi-2223 stability region. On the other hand, for samples annealed at high temperatures (A4), these new peaks are not appearing. Moreover, the Bi-2212 characteristic peak at 5.72° disappears, clearly indicating that the amount of Bi-2212 secondary phase decreases, compared with the unannealed samples.

Fig. 2 shows the SEM micrographs performed on the surfaces of all samples. From these images, it is clear that all samples possess large plate-like grains together with small ones which is a typical trademark of the classical solid state synthesis methods. Moreover, they show randomly oriented grains in all cases. When comparing the images obtained from the sintered samples with the annealed ones, the mean grain sizes seem to decrease when annealing is

performed. For samples A2 and A3 this evolution can be explained by the decomposition of Bi-2223 phase into Bi-2212 and Ca-Cu-O secondary phases which produces smaller size grains. In the case of A4 samples, it could be due to the formation of Bi-2223 phase from the smaller size secondary phases, leaving even smaller unreacted secondary phases as remains.

Fig. 3 shows the temperature dependence of the resistivity for all samples between 4.2 and 300 K. From this figure, it is clear that all samples show metallic behaviour above the T_c (onset). For the annealed samples, room temperature resistivity values decrease when the annealing temperature increases from A2 to A4. When taking into account the reference samples, A1, only samples A4 show lower room temperature resistivity. This evolution can be explained by the phases modification promoted by the annealing process. In the case of A2 and A3 samples, XRD data have shown an increase of Bi-2212 phase content with the annealing process. This effect is produced by the decomposition of Bi-2223 phase into Bi-2212 and the non-superconducting Ca-Cu-O secondary phase which is responsible for the increase of room temperature resistivity. On the other hand, for the A4 samples, powder XRD has shown a decrease on the Bi-2212 phase, indicating that this phase has reacted with some of the remaining non-superconducting Ca-Cu-O secondary phase to produce Bi-2223, explaining the lower room temperature resistivity. Other interesting feature that can be obtained from this figure is that the annealing process has nearly no influence on the T_c (offset) and very limited on the T_c (onset). This behaviour is easily explained when considering that the major phase in all the samples is the Bi-2223 and that the annealing processes have only produced very small changes in microstructure and phase composition. For

clarity, the T_c (onset) and T_c (offset) for all samples are displayed in Table I, together with the ΔT_c and room temperature resistivity values. In the table it can be observed that the modification of T_c (onset), produced by the annealing processes while the T_c (offset) is maintained practically constant, leads to ΔT_c values much higher for the annealed samples (A2, A3, and A4) than for the sintered ones (A1). The normal-to-superconducting state transition width strongly depends on the microstructure, grain links and the angles between grains [32-34]. As a consequence, the change on the transition width can be mainly due to the modifications in microstructure which can also promote small changes on the grain links, in agreement with the XRD and SEM data.

The investigation of the M-H hysteresis cycles at different temperatures is an important tool both for observing the energy required for destroying superconductivity completely [35]. Another important parameter obtained from M-H loops is M_R (remnant magnetization) values which provide important information about pinning strength [36].

The magnetic-hysteresis cycles, measured between applied fields of ± 2 T for all the samples, at 10 and 25 K are presented in Figs. 4 and 5, respectively. From these figures, it is clear that all samples show similar diamagnetic behaviour independently of the applied field and temperature. Moreover, when comparing with the values obtained for the sintered samples, M_R values and the area enclosed by the magnetization curve decrease for samples annealed at low temperatures (A2 and A3). On the other hand, these values are increased for samples annealed at high temperatures (A4). This evolution is in clear agreement with the XRD data which showed an increase on the Bi-2223 phase for samples A4, and with the electrical resistivity measurements showing a

decrease on the room temperature resistivity together with the higher T_c (onset and offset) values.

From these hysteresis-loops, the intragrain J_c values of the samples were determined using the Bean's model [37, 38]:

$$J_c = 30 \frac{\Delta M}{d}$$

where J_c is the magnetization current density in ampères per square centimeter.

$\Delta M = M_+ - M_-$ is measured in electromagnetic units per cubic centimeter, and d is the thickness of sample.

The magnetic field variation of J_c for all samples calculated at 10 K has been plotted in Fig. 6. From this figure, it is obvious that J_c values are very high and decrease with increasing the external magnetic applied field due to the weak links between grains [39]. However, these magnetically obtained critical current densities are higher than the transport critical current densities where the weak grain links and the grains orientation are also taken into account. The maximum J_c value of $\sim 7.8 \times 10^4$ A/cm² obtained for the A4 samples with no applied external field is about 10 % higher than the obtained for the sintered materials.

4. Conclusions

In summary, the effect of annealing temperatures on superconducting properties of bulk Bi-2223 ceramics with randomly oriented grains has been investigated. All the data have shown that annealing at low temperatures decrease the amount of Bi-2223 phase due to its decomposition into Bi-2212 and Ca-Cu-O secondary phases leading to lower superconducting properties than the sintered samples. On the other hand, high annealing temperatures increase the amount of Bi-2223 phase and improve the superconducting

properties. The maximum J_C values of $\sim 7.8 \times 10^4$ A/cm² obtained for these samples are about 10 % higher than the obtained for the sintered materials.

Acknowledgements

All samples have been prepared in the MEİTAM Central Laboratory in Mersin University in Turkey. SEM measurements have been made in the MEİTAM Central Laboratory in Mersin University, other measurements in this study have been made in the METU Central Laboratory in Middle East Technical University in Ankara in Turkey. On the other hand, I wish to thank M.Sc. Aynur GURBÜZ in the MEİTAM Central Laboratory and M.Sc. Ali GÜZEL, Dr. Ibrahim ÇAM in the METU Central Laboratory for their experimental support and very meticulous work.

M. A. Madre, J. C. Diez and A. Sotelo wish to thank the Gobierno de Aragón (Consolidated Research Groups T87 and T12) for financial support. M. A. Madre acknowledges the MINECO-FEDER (Project MAT2011-22719) for funding.

References

- [1] H. Maeda, Y. Tanaka, M. Fukutomi, T. Asano, Jpn. J. Appl. Phys. 27 (2) (1988) L209.
- [2] A. Sotelo, P. Majewski, H.S. Park, F. Aldinger, Physica C 272 (1996) 115.
- [3] A. Sotelo, G.F. de la Fuente, F. Lera, D. Beltran, F. Sapiña, R. Ibañez, A. Beltran, M. R. Bermejo, Chem. Mater. 5 (1993) 851.
- [4] T. Asaka, Y. Okazawa, T. Hirayama, K. Tachikawa, Jpn. J. Appl. Phys. 29 (1990) L280.
- [5] G. F. de la Fuente, A. Sotelo, Y. Huang, M.T. Ruiz, A. Badia, L. A. Angurel, F. Lera, R. Navarro, C. Rillo, R. Ibañez, D. Beltran, F. Sapiña, A. Beltran, Physica C 185 (1991) 509.

- [6] A. Sotelo, J.I. Peña, L. A. Angurel, J.C. Diez, M.T. Ruiz, G.F. de la Fuente, R. Navarro, *J. Mater. Sci.* 32 (1997) 5679.
- [7] M.A. Aksan, S. Altin, M.E. Yakinci, A. Guldeste, Y. Balci, *Mater. Sci. Technol.* 27 (2011) 314.
- [8] E. Barzi, V. Lombardo, D. Turrioni, F.J. Baca, T.G. Holesinger, *IEEE Trans. Appl. Supercond.* 21 (2011) 2335.
- [9] V. Garnier, R. Caillard, A. Sotelo, G. Desgardin, *Physica C* 319 (1999) 197.
- [10] S. Marinel, D. Bourgault, O. Belmont, A. Sotelo, G. Desgardin, *Physica C* 315 (1999) 205.
- [11] Y. Huang, G.F. de la Fuente, A. Sotelo, A. Badia, F. Lera, R. Navarro, C. Rillo, R. Ibañez, D. Beltran, F. Sapiña, A. Beltran, *Physica C* 185 (1991) 2401.
- [12] F.M. Costa, Sh. Rasekh, N.M. Ferreira, A. Sotelo, J.C. Diez, M.A. Madre, *J. Supercond. Nov. Magn.* 26 (2013) 943.
- [13] A. Sotelo, M.A. Madre, S. Rasekh, G. Constantinescu, M.A. Torres, J.C. Diez, *J. Supercond. Nov. Magn.* 26 (2013) 985.
- [14] M. Weigand, M. Eisterer, E. Giannini, H.W. Weber, *Phys. Rev. B* 81 (2010) 014516.
- [15] O. Bilgili, Y. Selamet, K. Kocabaş, *J. Supercond. Nov. Magn.* 21 (2008) 439.
- [16] H. Sözeri, N. Ghazanfari, H. Özkan, A. Kılıç, *Supercond. Sci. Technol.* 20 (2007) 522.
- [17] M. Mora, A. Sotelo, H. Amaveda, M.A. Madre, J.C. Diez, F. Capel, J. M. Lopez-Cepero, *J. Eur. Ceram. Soc.* 27 (2007) 3959.
- [18] L. Jiang, Y. Sun, X. Wan, K. Wang, G. Xu, X. Chen, K. Ruan, J. Du, *Physica C* 300 (1998) 61.

- [19] M. Zargar Shoushtari, S.E. Mousavi Ghahfarokhi, J. Supercond. Nov. Magn. 24 (2011) 1505.
- [20] A.I. Abou-Aly, M.M.H. Abdel Gawad, R. Awad, I. G-Eldeen, J. Supercond. Nov. Magn. 24 (2011) 2077.
- [21] M. Mora, A. Sotelo, H. Amaveda, M.A. Madre, J.C. Diez, L.A. Angurel, G.F. de la Fuente, Bol. Soc. Esp. Ceram. V. 44 (2005) 199.
- [22] S. Şakiroğlu, K. Kocabaş, J. Supercond. Nov. Magn. 24 (2011) 1321.
- [23] S.M. Khalil, J. Phys. Chem. Solids 62 (2001) 457.
- [24] A. Sotelo, M.A. Madre, J.C. Diez, Sh. Rasekh, L.A. Angurel, E. Martinez, Supercond. Sci. Technol. 22 (2009) 034012.
- [25] M.A. Madre, H. Amaveda, M. Mora, A. Sotelo, L.A. Angurel, J.C. Diez, Bol. Soc. Esp. Ceram. V. 47 (2008) 148.
- [26] Y.L. Chen, R. Stevens, J. Am. Ceram. Soc. 75 (1992) 1150.
- [27] R. Ramesh, S. Green, C. Jiang, Y. Mei, M. Rudee, H. Luo, G. Thomas, Phys. Rev. B 38 (1988) 7070.
- [28] B. Özkurt, M.A. Madre, A. Sotelo, J.C. Diez, J. Supercond. Nov. Magn. (2013) DOI: 10.1007/s10948-013-2193-5
- [29] A. Sotelo, L.A. Angurel, M.T. Ruiz, A. Larrea, F. Lera, G.F. de la Fuente, Solid State Ionics 63 (1993) 883.
- [30] S. Kaesche, P. Majewski, F. Aldinger, Z. Metallkd. 87 (1996) 587.
- [31] P. Majewski, S. Kaesche, F. Aldinger, J. Am. Ceram. Soc. 80 (1997) 1174.
- [32] D.A. Cardwell, A.D. Bradley, N.H. Babu, M. Kambara, W. Lo, Supercond. Sci. Technol. 15 (2002) 639.
- [33] Ph. Vanderdemden, A.D. Bradley, R.A. Doyle, W. Lo, D.M. Astill, D.A. Cardwell, A.M. Campbell, Physica C 302 (1998) 257.

- [34] U. Topal, M. Akdogan, J. Alloys Compounds 503 (2010) 1.
- [35] B. Özkurt, J. Mater Sci: Mater Electron (2012) doi: 10.1007/s10854-012-0806-6
- [36] B.A. Albiss, I.M. Obaidat, M. Gharaibeh, H. Ghamlouche, S.M. Obeidat, Solid State Commun. 150 (2010) 1542.
- [37] J.C. Bean, Phys. Rev. Lett. 8 (1962) 250.
- [38] B. Özkurt, M.A. Madre, A. Sotelo, J.C. Diez, J. Mater Sci: Mater Electron 24 (2013) 1158.
- [39] B. Özkurt, J. Supercond. Nov. Magn. 25 (2012) 1775.

Figure captions

Fig. 1. Powder XRD patterns of samples A1, A2, A3, and A4. Bi-2223 diffraction peaks are identified by *. The Bi-2212 peaks are shown by +.

Fig. 2. SEM micrographs obtained on fractured surfaces of (a) A1, (b) A2, (c) A3 and (d) A4 samples.

Fig. 3. Resistivity as a function of temperature curves for all the samples.

Fig. 4. Magnetization hysteresis curves between ± 2 T, measured at 10K for all samples

Fig. 5. Magnetization hysteresis curves between ± 2 T, measured at 25K for all samples.

Fig. 6. Calculated critical current densities for all the samples at 10K, as a function of the external applied field.

Table I. Resistivity measurement results for the samples

Samples	T_C^{onset} (K)	T_C^{offset} (K)	ΔT_C (K)	R(mohm.cm) at 300 K
A1	112	103	9	2.57
A2	120	102	18	3.91
A3	120	103	17	3.05
A4	122	105	17	2.29

Figure 1

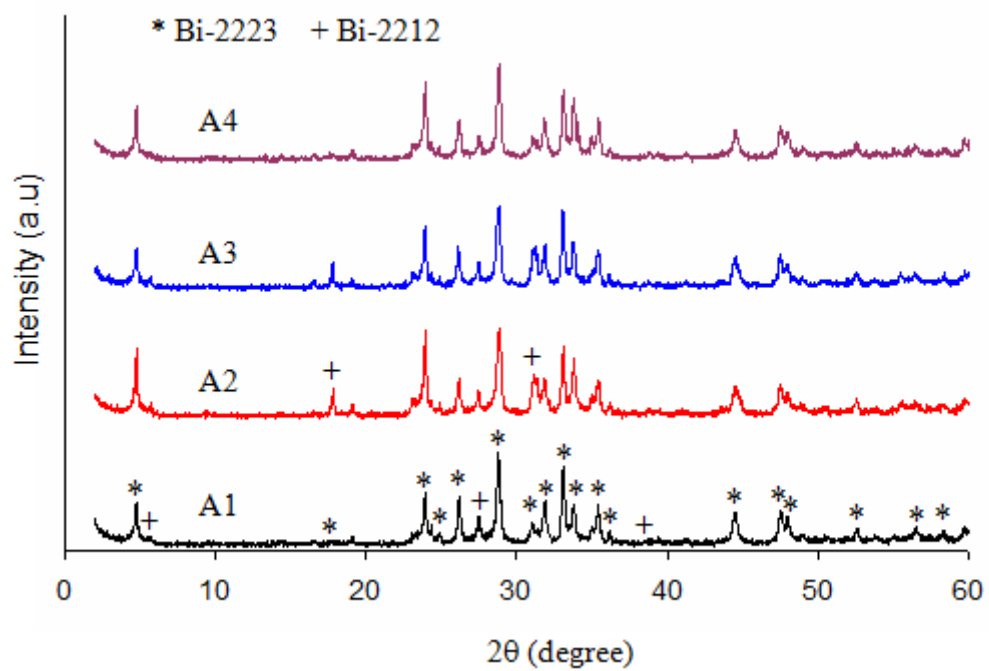
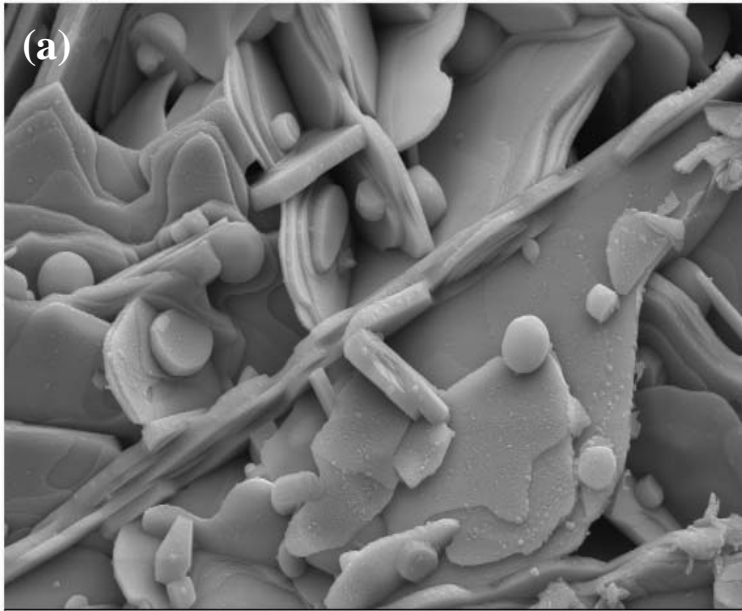
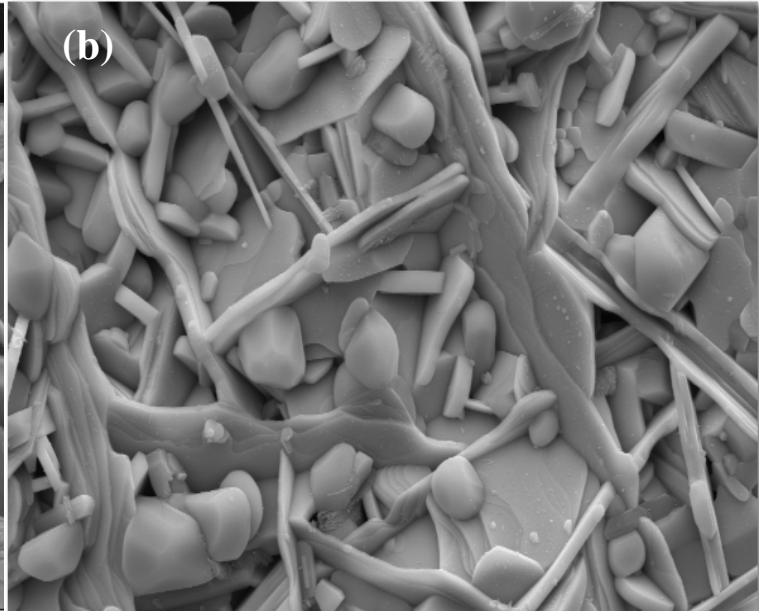


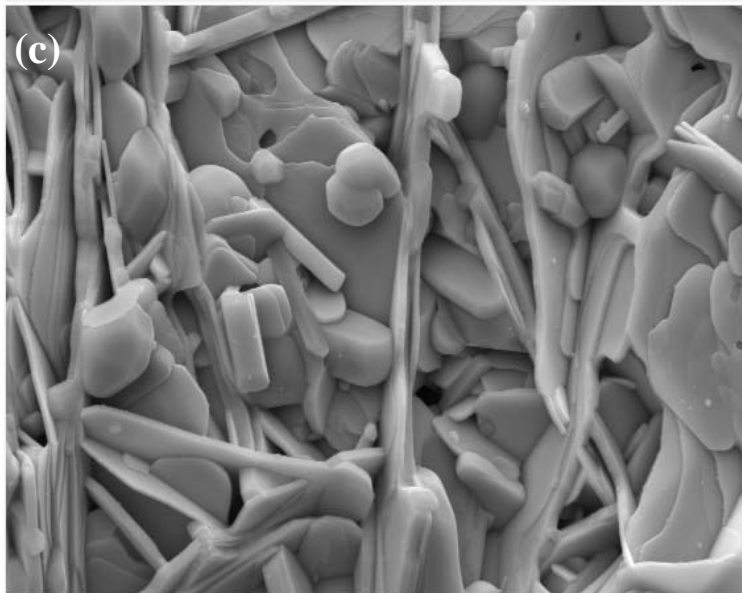
Figure 2



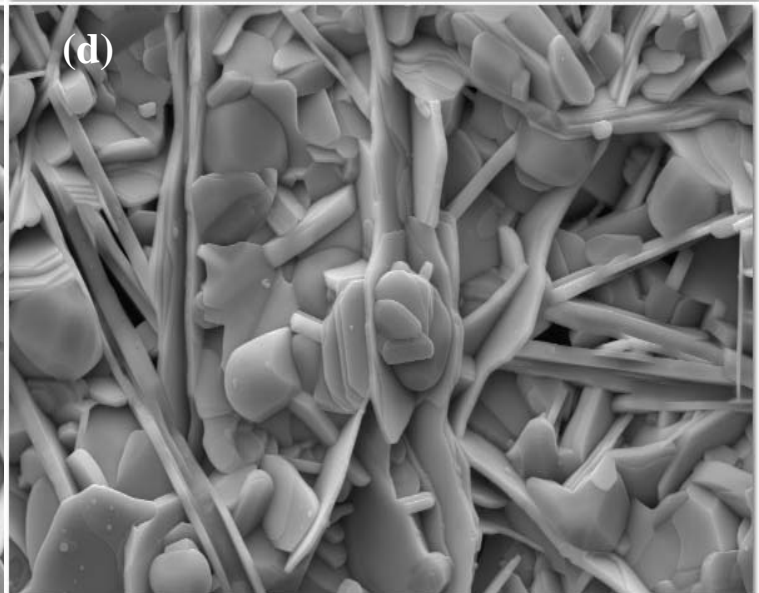
1 μ m EHT = 20.00 kV Signal A = SE2 Date :20 Nov 2012
WD = 11.0 mm Mag = 7.00 K X Time :15:51:20



1 μ m EHT = 20.00 kV Signal A = SE2 Date :20 Nov 2012
WD = 10.9 mm Mag = 7.00 K X Time :15:59:18



1 μ m EHT = 20.00 kV Signal A = SE2 Date :20 Nov 2012
WD = 11.0 mm Mag = 7.00 K X Time :16:07:29



1 μ m EHT = 20.00 kV Signal A = SE2 Date :20 Nov 2012
WD = 11.0 mm Mag = 7.00 K X Time :16:29:20



Figure 3

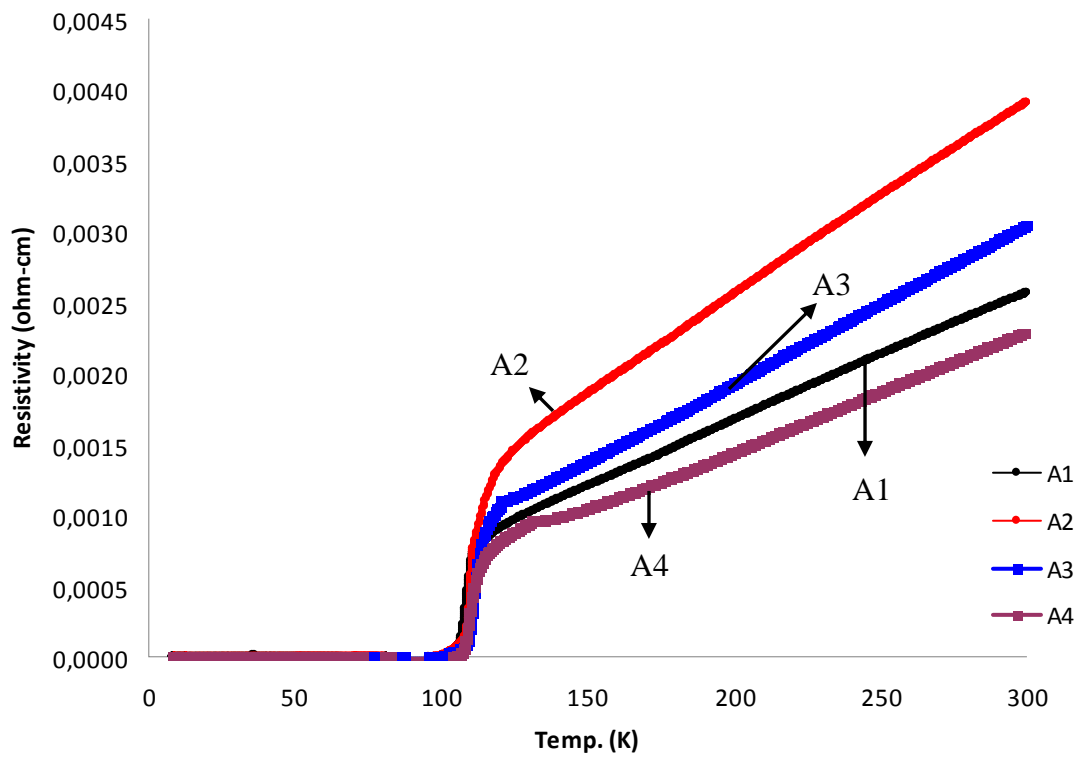


Figure 4

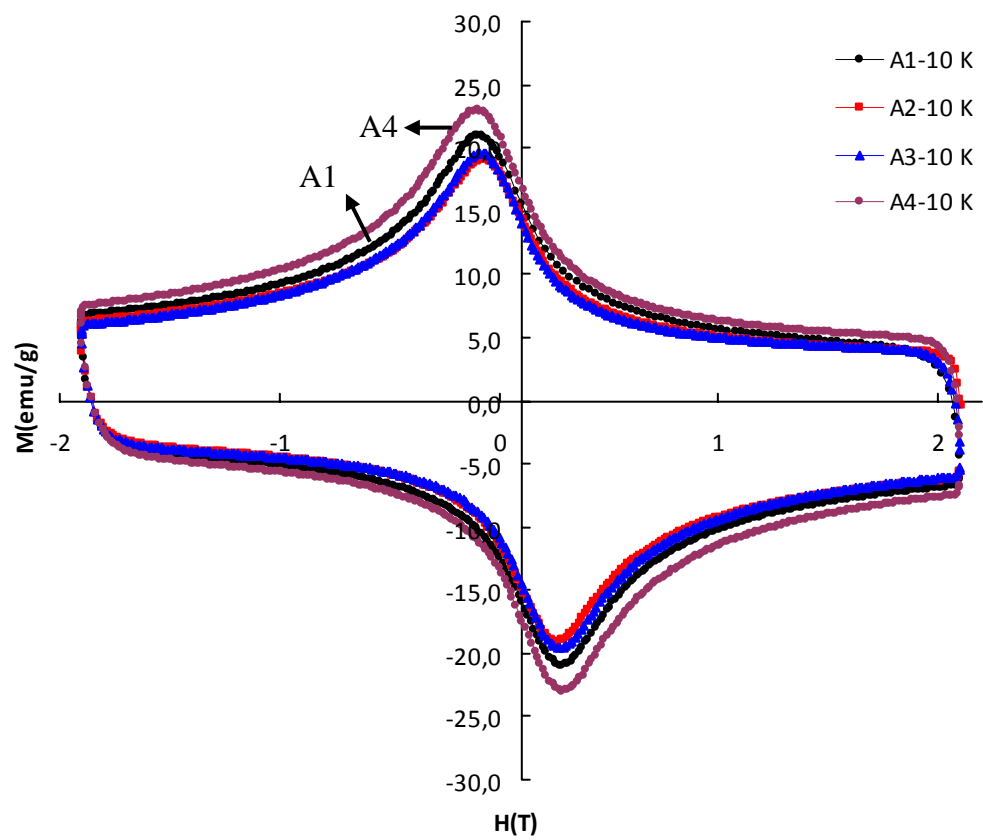


Figure 5

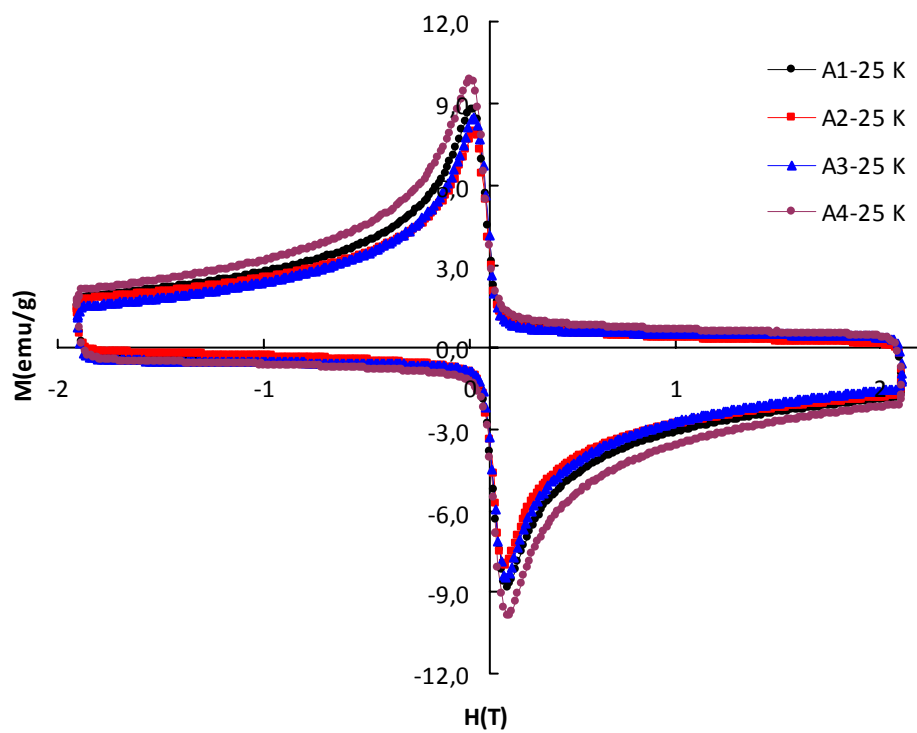


Figure 6

